Interaction of Vinca Alkaloids with Tubulin: A Comparison of Vinblastine, Vincristine, and Vinorelbine†

Sharon Lobert,*,‡ Bojana Vulevic,§ and John J. Correia§

School of Nursing and Department of Biochemistry, University of Mississippi Medical Center, Jackson, Mississippi 39216

Received December 21, 1995; Revised Manuscript Received April 3, 1996⊗

ABSTRACT: Vinca alkaloids are antimitotic drugs that inhibit microtubule assembly and induce tubulin self-association into coiled spiral aggregates. Previous sedimentation velocity results with vinblastine have been interpreted by a mechanism involving isodesmic ligand-mediated or ligand-mediated plus ligand-facilitated self-association [Lobert et al. (1995) *Biochemistry 34*, 8050−8060]. In this study, we compare the vincristine- or vinorelbine-induced self-association of porcine brain tubulin with our prior vinblastine studies in the presence of 50 μM GDP or 50 μM GTP. Vincristine demonstrates the highest overall affinity for tubulin, K_1K_2, and vinorelbine the lowest (vincristine > vinblastine > vinorelbine). These are the first quantitative studies comparing the interaction of a new vinca alkaloid derivative, vinorelbine (Navelbine), with other vinca alkaloids. The relative binding affinities reported here correlate with the weekly drug doses used clinically in cancer chemotherapy, where vincristine is used at the lowest dosages and vinorelbine at the highest. Surprisingly, K_1, the affinity of drug for tubulin heterodimers, is identical for all three drugs. When data are fit with the ligand-mediated model, the differences in overall affinity are due to effects on K_2, the affinity of liganded heterodimers for spiral polymers. When data are fit with the ligand-mediated plus -facilitated model, affinity differences are also reflected in K_3, the binding of the drug to unliganded polymers. We find that GDP enhances self-association in the presence of all three drugs 3−5-fold over GTP. The enhancement is manifested in K_2 and K_3 and amounts to an average of 0.90 ± 0.17 kcal/mol. Thus, nucleotide enhancement is linked to the self-association step. Data collected at 5, 25, and 36 °C for all three drugs show increased maximum $\bar{s}_{20,w}$ values with increasing temperature and are consistent with an entropically driven reaction for the overall process. To investigate these results further, stopped-flow light scattering experiments have been conducted. Relaxation times are longest for the largest vincristine polymers and shortest for the smallest vinorelbine polymers, consistent with a cascade of events corresponding to successive dissociation events from spiral polymers, the larger the polymers the longer the relaxation time. Relaxation times for any single drug decrease with increasing tubulin concentration, consistent with the occurrence of oligomer annealing in addition to the association of liganded heterodimers to the ends of the growing spirals. Relaxation times were used to estimate on and off rates for liganded heterodimer association with spirals, and their ratio gives affinity constants (K_{app}) that are independently consistent with K_2 estimates from sedimentation velocity results for vinblastine and vinorelbine. For vincristine-induced tubulin polymers, a two-step process is observed with a second relaxation time more than 20-fold longer than times observed for vinblastine or vinorelbine. Sedimentation velocity experiments at low speeds and electron microscopy are consistent with the presence of a small amount of larger polymers (≥40S) in the vincristine samples, possibly involving alignment of spirals. Under our experimental conditions, these larger polymers appear to have a minimal effect on the estimated energetics of the vincristine-induced self-association of tubulin.

Vinca alkaloids are important anticancer agents known to diminish microtubule dynamics and assembly, resulting in the arrest of cell division at metaphase. They are used clinically for a variety of hematologic and solid tumors. At substoichiometric levels, *in vitro*, vinca alkaloids are known to stabilize microtubules, possibly by binding to microtubule ends and inhibiting hydrolysis of GTP (Toso et al., 1993; Jordan et al., 1991; Jordan & Wilson, 1990). Stoichiometric drug concentrations result in extensive microtubule depolymerization, and in the presence of MAPs or at high magnesium concentrations (>2.5 mM) or high ionic strengths, large paracrystals form (Na & Timasheff, 1986b). These paracrystals are believed to be made up of spiral helices of one or two protofilaments that align to form "macrotubes" (Fujiwara & Tilney, 1975; Amos et al., 1984; Himes, 1991; Nogales et al., 1995).

The interactions of vinblastine with tubulin heterodimers and microtubules have been studied extensively, and *in vitro* studies have shown that at low ionic strengths vinblastine induces spiral formation by a mechanism involving ligand-

† This work was supported by Grants NR00056 (S. L.) from NIH and BIR9216150 (J. J. C.) from NSF.

* To whom correspondence should be addressed: School of Nursing, University of Mississippi Medical Center, 2500 N. State St., Jackson, MS 39216. Phone: 601-984-6217.

‡ School of Nursing.

§ Department of Biochemistry.

⊗ Abstract published in *Advance ACS Abstracts,* May 15, 1996.

[1] Abbreviations: EGTA, [ethylenebis(oxyethylenenitrilo)]tetraacetic acid; MAP, microtubule-associated protein; PC-tubulin, MAP-free phosphocellulose-purified tubulin; Pipes, piperazine-*N*,*N*′-bis(2-ethanesulfonic acid).

S0006-2960(95)03037-6 CCC: $12.00

mediated plus ligand-facilitated isodesmic self-association (Na & Timasheff, 1982, 1986b; Himes, 1991). We have recently shown that GDP enhances vinblastine-induced spiral formation (Lobert et al., 1995). Vincristine is known to bind to tubulin with higher overall affinity than vinblastine (Owellen et al., 1972; Prakash & Timasheff, 1983, 1985) and at substoichiometric concentrations induces the formation of spiral polymers similar to those found in the presence of vinblastine (Na & Timasheff, 1982). It has also been observed that at neutral pH vincristine more readily induces a tubulin "denatured" state than vinblastine (Prakash & Timasheff, 1992). Vincristine at stoichiometric concentrations induces formation of paracrystalline aggregates similar to those formed in the presence of vinblastine (Na & Timasheff, 1982). Immunofluorescence studies of vinorelbine, a newer semisynthetic vinca alkaloid analog, have shown that it interacts with mitotic microtubules with an effect similar to that of vincristine and vinblastine, although higher concentrations are required (Binet et al., 1990). Although vinorelbine is known to cause paracrystal formation at stoichiometric concentrations (Fellous et al., 1989), little is known about the energetics of vinorelbine-induced spiral formation.

In the work described here, we compare vincristine-, vinblastine-, and vinorelbine-induced tubulin self-association using sedimentation velocity in the presence of GDP or GTP. These are the first quantitative studies comparing the interaction of a new vinca alkaloid derivative, vinorelbine (Navelbine), with other vinca alkaloids. These studies address the hypothesis that GDP enhances tubulin self-association in the presence of other vinca alkaloids besides vinblastine (Lobert et al., 1995). We find the order of overall binding affinity to be vincristine > vinblastine > vinorelbine. All three drugs bind with nearly identical affinity to tubulin heterodimers, K_1. The major difference in binding is in K_2, the affinity of liganded heterodimers for polymers. When data are fit with the combined ligand-mediated plus -facilitated model, K_3, the binding of drug to unliganded polymer, is enhanced (Na & Timasheff, 1986b; Lobert et al., 1995). In addition, we find, consistent with our hypothesis, that GDP enhances tubulin self-association 3−5-fold over GTP for all three drugs. Data collected at 5, 25, and 36 °C for all three drugs show an increased maximum $\bar{s}_{20,w}$ with increasing temperature, consistent with an entropically driven reaction for the overall process. We also investigated the mechanism for vinca alkaloid-induced tubulin association by stopped-flow light scattering. We find that the relaxation times, τ, are longest for the largest vincristine polymers and shortest for the smallest vinorelbine polymers. Additionally, there is a decrease in τ with increasing tubulin concentration, suggesting annealing of oligomers in addition to association of liganded heterodimers (Thusius et al., 1975; Nogales et al., 1995).

MATERIALS AND METHODS

Reagents. Deionized (Nanopure) water was used in all experiments. $MgSO_4$, EGTA, GDP (type I), GTP (type II-S), and Pipes were purchased from Sigma Chemical Co. Sephadex G-50 was from Pharmacia. Vinblastine sulfate and vincristine sulfate were from Sigma, and vinorelbine ditartrate was from Glaxo Wellcome, Inc.

Tubulin Purification. Porcine brain tubulin (PC-tubulin) free of MAPs was obtained by two cycles of warm−cold polymerization−depolymerization followed by phosphocellulose chromatography to separate tubulin from MAPs (Williams & Lee, 1982; Correia et al., 1987). Protein concentrations were determined spectrophotometrically (Detrich & Williams, 1978) (E_{278} = 1.2 L g^{-1} cm^{-1}).

Sedimentation Velocity Experiments. Sedimentation studies were done in a Beckman Optima XLA analytical ultracentrifuge equipped with absorbance optics and an An60 Ti rotor. Self-association of PC-tubulin (2 μM) in the presence of vinblastine, vincristine, or vinorelbine and GDP or GTP was studied by sedimentation velocity. Tubulin samples were equilibrated in 10 mM Pipes (pH 6.9), 2 mM EGTA, 1 mM $MgSO_4$, and 50 μM GXP using spun columns as described previously (Lobert et al., 1995). These equilibration procedures take advantage of the magnesium dependence of GTP binding to tubulin and ensure that samples are >99% pure GDP−tubulin or GTP−tubulin (Correia et al., 1987; Lobert et al., 1995). The free drug concentration (0.05−70 μM) was obtained from the known drug concentration in the equilibration buffer. After equilibration, the protein was brought to the desired final concentration by dilution with the equilibration buffer. Samples were spun in a Beckman XLA analytical ultracentrifuge at 5, 25, or 36 °C and 30 000 or 42 000 rpm. Temperature was calibrated by the method of Liu and Stafford (1995). Velocity data were collected at 280 nm and at a spacing of 0.01 cm with four averages in a continuous scan mode. Data were analyzed using software (DCDT) provided by Dr. Walter Stafford (Boston Biomedical Research Institute) to generate a distribution of sedimentation coefficients, $g(s)$, as described previously (Lobert et al., 1995).

Curve Fitting of Sedimentation Velocity Data. The sedimentation data were plotted as weight average $\bar{s}_{20,w}$ vs free drug concentration. Total protein concentration in the plateau was determined from $\int g(s)\,ds$. Sedimentation data were fit using the isodesmic ligand-mediated or isodesmic ligand-mediated plus -facilitated model (also referred to as the combined model) as previously described (Lobert et al., 1995). In these models, K_1 is the affinity of drug for tubulin heterodimers, K_2 is the affinity of liganded heterodimers for spiral polymers, K_3 is the affinity of drug for polymers, and K_4 is the association constant for unliganded tubulin heterodimers. Binding constants were obtained by fitting with the nonlinear least squares program Fitall (MTR software, Toronto, Canada), modified to include the appropriate fitting functions.

Stopped-Flow Light Scattering Experiments. PC-Tubulin (1−4 μM) was equilibrated, using spun columns, into 10 mM Pipes (pH 6.9), 2 mM EGTA, 1 mM $MgSO_4$, and 50 μM GTP and 50 μM vinorelbine, vinblastine, or vincristine. Samples were degassed for 1 h at room temperature. Stopped-flow rapid mixing experiments (Hi Tech manual stopped-flow apparatus) were initiated by diluting tubulin samples 1:1 with the same buffer without drug, with a dead time of 1 s. The final drug and tubulin concentrations were 25 and 0.5−2 μM, respectively. Relaxation was monitored using a SLM Aminco Bowman Series 2 Luminescence Spectrometer at 350 nm (90° scattering) over 10 min for vinorelbine and vinblastine and over 30−45 min for vincristine at 1 s intervals. Data were fit using Origin 3.5, to obtain relaxation times, τ, using the following equation, $x = a_0 \exp(-t/\tau)$, where a_0 is the change in amplitude associated with τ over time, t (seconds) (Bernasconi, 1976).

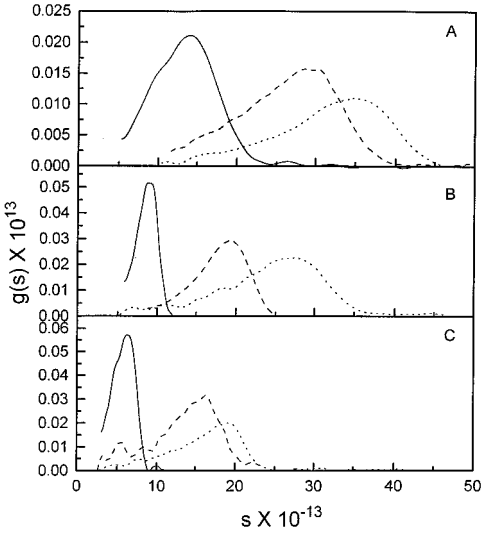

FIGURE 1: Sedimentation coefficient distribution, $g(s)$, plots of ligand-induced tubulin self-association in the presence of 30 μM drug at 5 (—), 25 (---), and 36 (···) °C. All data were collected in the presence of 50 μM GTP and 2 μM tubulin: (A) vincristine, (B) vinblastine, and (C) vinorelbine. The vinblastine data are from Lobert et al. (1995) and are reproduced here in a new format for clarity of presentation.

Alternatively, two relaxation times, τ_1 and τ_2, were determined by fitting data with the summation $x = a_1 \exp(-t/\tau_1) + a_2 \exp(-t/\tau_2)$, where a_1 and a_2 are the amplitude changes associated with τ_1 and τ_2. Chi-square determinations were used to select the best fits of the data. In order to calculate the on rate, k_a, and the off rate, k_d, for vinblastine and vinorelbine, $1/\tau^2$ was plotted against the final tubulin concentration. The data were then fit by linear regression and the slope and y-intercept used to determine k_a and k_d (Thusius et al., 1975). As described below, the vincristine kinetic data were more complex, and therefore, k_a and k_d could not be estimated in this way.

Electron Microscopy. Tubulin (4 μM) samples were prepared at room temperature in the presence of 50 μM vincristine in 10 mM Pipes (pH 6.9), 2 mM EGTA, 1 mM $MgSO_4$, and 50 μM GTP. The method used for glutaraldehyde fixation and negative staining with uranyl acetate has been described previously (Lobert et al., 1995).

RESULTS

Sedimentation Velocity Experiments. The association of 2 μM PC-tubulin in the presence of vincristine, vinblastine, or vinorelbine, ranging from 0.05 to 70 μM, and 50 μM GDP or 50 μM GTP was studied by sedimentation velocity at 5, 25, or 36 °C. Figure 1 shows sedimentation coefficient distributions, $g(s)$, calculated from the sedimenting boundary (Stafford, 1992a,b, 1994) for data collected in the presence of GTP. We find that increasing the temperature results in larger $\bar{s}_{20,w}$ values for vinorelbine and vincristine. These data agree with our previous findings for vinblastine (Lobert et al., 1995) and are consistent with an entropically driven process. Data collected in the presence of GDP demonstrated a similar temperature dependence, although the maximum s values were larger than in the presence of GTP. This enhancement of drug-induced tubulin self-association by GDP is shown in Figure 2. Weight average sedimentation coefficients were calculated from the $g(s)$ data and plotted against free drug concentrations for 36 °C data. The solid

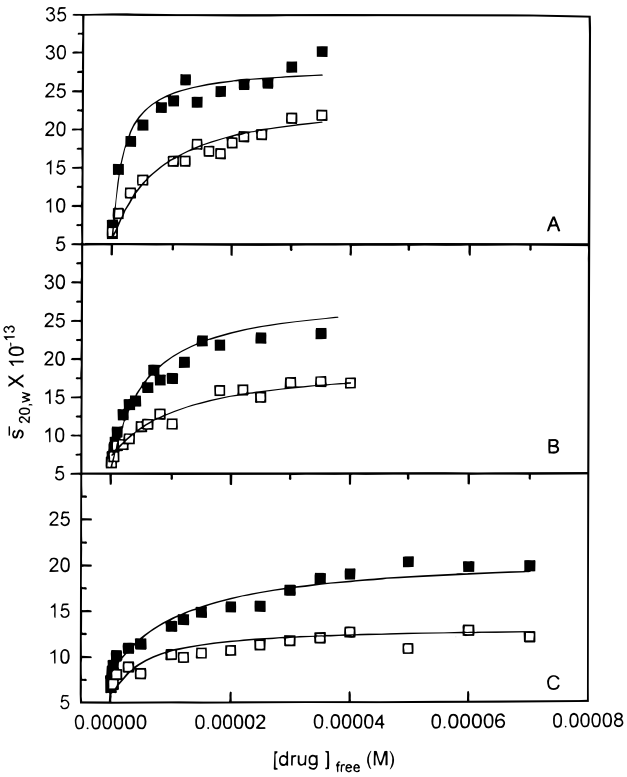

FIGURE 2: Plots of $\bar{s}_{20,w}$ values vs free vincristine, vinblastine, or vinorelbine concentrations at 36 °C. Tubulin in all experiments was 2 μM in the presence of 50 μM GTP (□) or GDP (■). The solid lines represent fits using the ligand-mediated model. The panels show tubulin self-association induced by (A) vincristine, (B) vinblastine, or (C) vinorelbine. The vinblastine data are from Lobert et al. (1995) and are reproduced here in a new format for clarity of presentation.

lines in Figure 2 represent ligand-mediated fits of the data. It can be seen that the maximum $\bar{s}_{20,w}$ values in the presence of GDP are larger than in the presence of GTP. When the vincristine data were compared with our previous vinblastine data, vincristine was found to induce the largest species, with a maximum $\bar{s}_{20,w}$ of 30S in the presence of GDP and 22S in the presence of GTP. Vinorelbine was found to induce the smallest species, with a maximum $\bar{s}_{20,w}$ value of 20S and 13S for GDP and GTP, respectively. The maximum $\bar{s}_{20,w}$ for vinblastine was 23S and 17S for GDP and GTP conditions, respectively.

Table 1 shows the binding affinities for vincristine and vinorelbine obtained from fitting with the ligand-mediated or ligand-mediated plus -facilitated models. The combined model resulted in identical or slightly improved fits for all data. As discussed in our previous work (Lobert et al., 1995), it is necessary to constrain K_4, the association constant for unliganded tubulin heterodimers, to 1×10^4 M^{-1} in order to compare the binding affinities, since only three binding constants are independent in this scheme. The constrained and unconstrained fits are listed in Table 1 for comparison with one another and with previous vinblastine results (Lobert et al., 1995; Na & Timasheff, 1986b; Prakash & Timasheff, 1983, 1985). It should be noted that when data are fit with the ligand-mediated model the effect of GDP occurs primarily on K_2, the affinity for association of liganded heterodimers, rather than on K_1, the affinity for drug binding to the heterodimer. This is in agreement with the GDP enhancement found in the presence of vinblastine (Lobert et al., 1995). For example, at 25 °C, the average value for

Table 1: Equilibrium Constants for the Interaction of Vinca Alkaloids with Tubulin

drug	T (°C)	GXP	K_1 (M^{-1})	K_2 (M^{-1})	K_3 (M^{-1})	K_1K_2 (M^{-2})	SD
vincristine	5	GTP	$3.4 \times 10^5 \pm 0.8$	$8.0 \times 10^6 \pm 0.4$		2.7×10^{12}	1.0[a]
			$2.7 \times 10^5 \pm 0.1$	$2.9 \times 10^5 \pm 0.1$	$7.7 \times 10^6 \pm 0.2$	7.7×10^{10}	1.0[b]
			$2.3 \times 10^5 \pm 0.8$	$4.6 \times 10^5 \pm 4.7$	$4.5 \times 10^6 \pm 4.0$	1.1×10^{11}	1.0[c]
		GDP	$2.4 \times 10^5 \pm 0.5$	$4.0 \times 10^7 \pm 0.5$		9.5×10^{12}	1.5[a]
			$2.2 \times 10^5 \pm 0.2$	$6.4 \times 10^5 \pm 1.2$	$1.4 \times 10^7 \pm 0.1$	1.4×10^{11}	1.5[b]
			$2.0 \times 10^5 \pm 0.5$	$1.3 \times 10^6 \pm 3.0$	$6.6 \times 10^6 \pm 6.5$	2.7×10^{11}	1.5[c]
	25	GTP	$1.4 \times 10^5 \pm 0.4$	$1.7 \times 10^7 \pm 0.4$		2.3×10^{12}	1.2[a]
			$1.3 \times 10^5 \pm 0.1$	$4.1 \times 10^5 \pm 0.8$	$5.2 \times 10^6 \pm 0.4$	5.2×10^{10}	1.1[b]
			$1.3 \times 10^5 \pm 0.5$	$1.1 \times 10^6 \pm 0.8$	$1.7 \times 10^6 \pm 0.8$	1.4×10^{11}	0.9[c]
		GDP	$2.1 \times 10^5 \pm 0.4$	$3.9 \times 10^7 \pm 0.5$		7.9×10^{12}	1.7[a]
			$1.9 \times 10^5 \pm 0.3$	$6.1 \times 10^5 \pm 3.4$	$1.2 \times 10^7 \pm 0.3$	1.2×10^{11}	1.7[b]
			$1.7 \times 10^5 \pm 0.6$	$1.1 \times 10^6 \pm 2.1$	$6.2 \times 10^6 \pm 6.0$	1.9×10^{11}	1.4[c]
	36	GTP	$1.3 \times 10^5 \pm 0.3$	$1.1 \times 10^7 \pm 0.2$		1.5×10^{12}	0.9[a]
			$1.1 \times 10^5 \pm 0.1$	$3.5 \times 10^5 \pm 0.5$	$3.9 \times 10^6 \pm 0.2$	3.9×10^{10}	0.8[b]
			$1.1 \times 10^5 \pm 0.2$	$1.0 \times 10^6 \pm 0.4$	$1.1 \times 10^6 \pm 0.2$	1.2×10^{11}	0.4[c]
		GDP	$4.8 \times 10^5 \pm 1.2$	$2.0 \times 10^7 \pm 0.2$		9.4×10^{12}	1.6[a]
			$4.5 \times 10^5 \pm 0.1$	$4.4 \times 10^5 \pm 0.3$	$2.0 \times 10^7 \pm 0.1$	2.0×10^{11}	1.6[b]
			$5.8 \times 10^5 \pm 0.4$	$1.0 \times 10^6 \pm 0.2$	$9.5 \times 10^6 \pm 0.6$	5.8×10^{11}	1.1[c]
vinorelbine	5	GTP	$1.1 \times 10^5 \pm 0.2$	$7.2 \times 10^5 \pm 0.9$		7.6×10^{10}	0.3[a]
			$7.8 \times 10^4 \pm 2.0$	$9.5 \times 10^4 \pm 5.3$	$7.3 \times 10^5 \pm 2.0$	7.3×10^9	0.4[b]
			$9.7 \times 10^4 \pm 1.8$	$2.4 \times 10^4 \pm 1.1$	$3.0 \times 10^6 \pm 0.6$	2.3×10^9	0.3[c]
		GDP	$1.2 \times 10^5 \pm 0.2$	$4.1 \times 10^6 \pm 0.5$		4.7×10^{11}	0.8[a]
			$8.6 \times 10^4 \pm 2.8$	$1.9 \times 10^5 \pm 1.6$	$1.6 \times 10^6 \pm 0.6$	1.6×10^{10}	1.2[b]
			$6.1 \times 10^4 \pm 1.6$	$5.3 \times 10^5 \pm 5.1$	$6.2 \times 10^6 \pm 3.0$	3.2×10^{10}	0.6[c]
	25	GTP	$2.3 \times 10^5 \pm 0.6$	$1.5 \times 10^6 \pm 0.2$		2.8×10^{11}	0.6[a]
			$1.7 \times 10^5 \pm 0.6$	$1.2 \times 10^5 \pm 2.6$	$2.1 \times 10^6 \pm 2.4$	2.1×10^{10}	0.6[b]
			$1.7 \times 10^5 \pm 0.5$	$1.3 \times 10^5 \pm 1.6$	$2.1 \times 10^6 \pm 1.3$	2.3×10^{10}	0.6[c]
		GDP	$1.8 \times 10^5 \pm 0.4$	$6.7 \times 10^6 \pm 0.7$		1.2×10^{12}	1.0[a]
			$1.5 \times 10^5 \pm 0.3$	$2.4 \times 10^5 \pm 1.7$	$3.6 \times 10^6 \pm 1.2$	3.6×10^{10}	1.4[b]
			$1.1 \times 10^5 \pm 0.2$	$7.8 \times 10^5 \pm 5.1$	$1.1 \times 10^6 \pm 0.4$	8.7×10^{10}	0.8[c]
	36	GTP	$2.3 \times 10^5 \pm 0.9$	$2.0 \times 10^6 \pm 0.3$		4.7×10^{11}	1.1[a]
			$1.8 \times 10^5 \pm 0.3$	$1.4 \times 10^5 \pm 0.4$	$2.6 \times 10^6 \pm 0.3$	2.6×10^{10}	1.1[b]
			$3.4 \times 10^4 \pm 3.4$	$1.0 \times 10^6 \pm 1.4$	$1.4 \times 10^5 \pm 1.2$	3.4×10^{10}	0.9[c]
		GDP	$2.3 \times 10^5 \pm 0.6$	$8.1 \times 10^6 \pm 1.0$		1.8×10^{12}	1.4[a]
			$2.1 \times 10^5 \pm 0.2$	$2.8 \times 10^5 \pm 0.6$	$6.0 \times 10^6 \pm 0.5$	6.0×10^{10}	1.3[b]
			$1.2 \times 10^5 \pm 0.4$	$1.7 \times 10^6 \pm 0.9$	$5.7 \times 10^5 \pm 2.0$	2.0×10^{11}	0.7[c]

[a] Data were fit with the ligand-mediated model. [b] Data were fit with the combined ligand-mediated plus -facilitated model and K_4 was constrained to be 1×10^4 M^{-1}. [c] Data were fit with an unconstrained combined ligand-mediated plus -facilitated model.

K_1 (M^{-1}), obtained from all models, for vincristine is 1.6×10^5 (± 0.3) and for vinorelbine is 1.7×10^5 (± 0.4). Similarly, for vinblastine, the average K_1 (M^{-1}) was found to be 1.4×10^5 (± 0.3) (Lobert et al., 1995). K_2 is more model- and nucleotide-dependent, but the enhancement by drug or nucleotide is evident in K_2 for all cases. For example, for vincristine data, at 25 °C, fit with the constrained combined model, K_2 (M^{-1}) is 4.1×10^5 and 6.1×10^5, for GTP and GDP, respectively. When the same data are fit with the ligand-mediated model, K_2 (M^{-1}) is 1.7×10^7 and 3.9×10^7 for GTP and GDP, respectively. Similarly, for vinorelbine data, at 25 °C, fit with the combined model, K_2 (M^{-1}) is 1.2×10^5 and 2.4×10^5 for GTP and GDP, respectively. When the data are fit with the ligand-mediated model, the values (M^{-1}) are 1.5×10^6 and 6.7×10^6 for GTP and GDP data, respectively. Additionally, for the combined model, the GDP enhancement is also found in K_3, the affinity of drug for unliganded polymers. Thus, this enhancement is clearly linked to tubulin self-association. The overall affinity, K_1K_2, for all three drugs is enhanced 3−5-fold when GDP is present compared to when GTP is present. This enhancement ranges from 0.69 to 1.13 kcal/mol, with a mean value of 0.90 ± 0.17 kcal/mol. The overall binding affinities, K_1K_2, regardless of the nucleotide present, demonstrate that in order of magnitude vincristine > vinblastine > vinorelbine.

Table 2: Thermodynamic Parameters for Tubulin-Vinca Alkaloid Interaction at 25 °C

	K_1K_2 (M^{-2})	$\Delta G°$ (kcal/mol)	$\Delta S°$ (cal mol^{-1} K^{-1})	$\Delta H°$ (kcal/mol)
Ligand-Mediated plus -Facilitated Model (Constrained)				
		Vinorelbine		
GTP	2.1×10^{10}	−14.1	72	7.3
GDP	3.6×10^{10}	−14.4	74	7.2
		Vinblastine[a]		
GTP	2.3×10^{10}	−14.1	77	8.7
GDP	5.8×10^{10}	−14.7	58	2.5
		Vincristine		
GTP	5.2×10^{10}	−14.6	37	−3.7
GDP	1.2×10^{11}	−15.1	47	1.5
Ligand-Mediated Model				
		Vinorelbine		
GTP	2.8×10^{11}	−15.6	87	10.2
GDP	1.2×10^{12}	−16.5	80	7.4
		Vinblastine[a]		
GTP	6.1×10^{11}	−16.1	68	4.2
GDP	3.0×10^{12}	−17.0	64	2.0
		Vincristine		
GTP	2.3×10^{12}	−16.9	47	−2.9
GDP	7.9×10^{12}	−17.6	60	−0.26

[a] Vinblastine data from Lobert et al. (1995) reproduced here for clarity of presentation.

Table 2 shows the thermodynamic parameters obtained from van't Hoff plots (data not shown) of the vinorelbine, vinblastine, and vincristine data fit with the ligand-mediated and combined models. For all three drugs, $\Delta G°$ is more

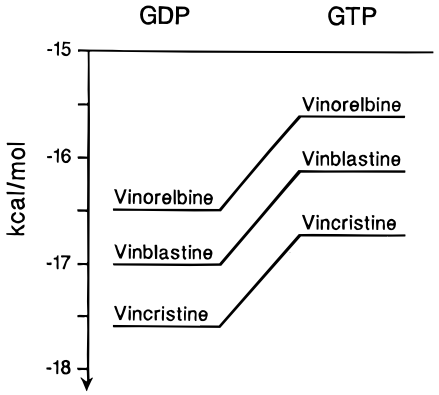

FIGURE 3: Plot of the relationship of the overall free energy of drug-induced association in the presence of GDP or GTP. Data collected at 25 °C were fit with the ligand-mediated model. The GDP enhancement equals 0.90 (±0.17) kcal/mol for all three drugs. Vincristine-induced tubulin association is the most favorable, and vinorelbine-induced tubulin association is the least favorable.

negative in the presence of GDP than in the presence of GTP. This difference is most evident when the data are fit with the ligand-mediated model. Figure 3 gives a graphical representation of the GDP enhancement in terms of overall free energy of association, using parameters obtained from the ligand-mediated fits at 25 °C. The overall free energy change, $\Delta G°$, for vincristine-induced tubulin association in the presence of GDP is −17.6 kcal/mol compared to −16.9 kcal/mol in the presence of GTP. Similarly, $\Delta G°$ values for vinblastine and vinorelbine-induced tubulin association in the presence of GDP are −17.0 and −16.5 kcal/mol, respectively, compared to −16.1 and −15.6 kcal/mol, respectively in the presence of GTP. In all three cases, the overall free energy at 25 °C is more negative in the presence of GDP than in the presence of GTP by an average of 0.83 ± 0.12 kcal/mol (averaged over all temperatures, 0.90 ± 0.17 kcal/mol). The $\Delta H°$ and $\Delta S°$ values are consistent with an entropically driven polymerization process, although the absolute values are model-dependent. The unfavorable $\Delta H°$ in general is compensated by a positive $\Delta S°$, regardless of the model used to fit the data. The only favorable $\Delta H°$ values are found in the vincristine data (Table 2; see Discussion).

Stopped-Flow Light Scattering. In order to investigate the kinetics of drug-induced tubulin association, we used rapid mixing stopped-flow light scattering, where each drug was diluted from 50 to 25 μM at 25 °C and the final tubulin concentration varied from 0.5 to 2 μM. Figure 4 presents examples of typical relaxation traces observed over 600 s for each drug. The final tubulin concentration for these experiments was 1.5 μM. It can be seen that the relaxation data for vinorelbine and vinblastine appear quite similar. These data can be fit well with single exponentials to obtain relaxation times. Table 3 presents the relaxation data for vinorelbine and vinblastine at 0.5, 1.0, and 1.5 μM tubulin. In this table, A1 represents the change in the light scattering signal and τ_1 is the relaxation time in seconds. It should be noted that vinorelbine relaxation times are shorter than those of vinblastine (range from 7.56 to 12.77 s vs 19.97 to 34.60 s, respectively). This is consistent with a model that involves a cascade of dissociation events from larger to smaller polymers upon dilution. The larger polymer distribution for vinblastine vs vinorelbine (Figures 1 and 2) is consistent with these longer average relaxation events for vinblastine.

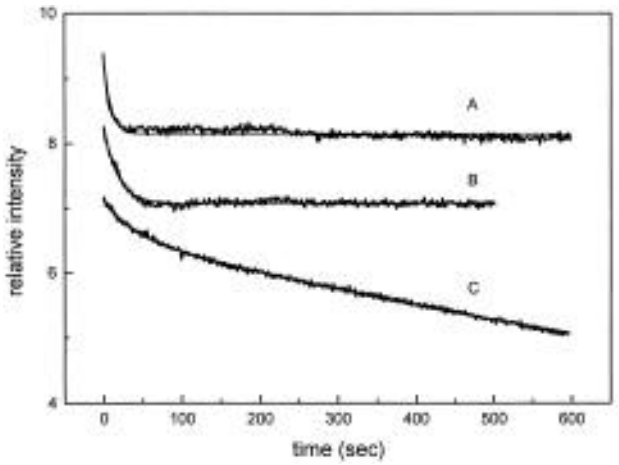

FIGURE 4: Stopped-flow light scattering experiments. Relative intensity is plotted vs time (seconds). As described in Materials and Methods, the drug concentrations were initially 50 μM. Following dilution to 25 μM drug, scattering was monitored over 10 min at 1 s intervals: (A) vinorelbine, (B) vinblastine, and (C) vincristine.

Furthermore, the relaxation time decreases with increasing tubulin concentration. This result suggests that, in addition to liganded heterodimers adding to or dissociating from polymers, oligomers can self-associate or dissociate in a mechanism consistent with annealing of spiral polymers. This has been observed previously in the relaxation data for glutamate dehydrogenase (Thusius et al., 1975) and has been suggested to occur for vinblastine spirals during temperature jump experiments (Nogales et al., 1995). Note that this complexity in the kinetics does not obviate the equilibrium analysis by a combined ligand-mediated plus -facilitated mechanism because the overall thermodynamics are path-independent and still describe the final equilibrium distribution.

To obtain the on rate, k_a, and the off rate, k_d, for vinorelbine and vinblastine, the squares of the reciprocals of the relaxation times ($1/\tau^2$) were plotted against the final tubulin concentrations (Table 4). Vinorelbine has a slower k_d than vinblastine, 0.0210 and 0.0082 s^{-1}, respectively. In addition, k_a is smaller for vinorelbine than for vinblastine, 1.1×10^5 and 4.2×10^5 M^{-1} s^{-1}, respectively. The binding affinities were determined from the ratio k_a/k_d to be 5.4×10^6 M^{-1} for vinorelbine and 5.2×10^6 M^{-1} for vinblastine. The result for vinblastine is in excellent agreement with the K_2 determined by sedimentation velocity, 5.1×10^6 M^{-1} (Lobert et al., 1995). The kinetically calculated binding affinity of vinorelbine also agrees reasonably well with the sedimentation result, 1.5×10^6 M^{-1}. We conclude that the stopped-flow kinetic data are accurate indicators of polymer redistribution events involving self-association/dissociation rates and independently verify K_2, the affinity of liganded heterodimers for growing polymers.

The vincristine relaxation times are considerably longer and more complex, requiring two relaxation events to fit the data (Figure 4, Table 3). In a manner similar to that of vinorelbine and vinblastine, the relaxation times demonstrate a decreasing trend with increasing tubulin concentration, although within the error of the measurement, the trend is less certain. The average τ_1 and τ_2 values were found to be 92.76 ± 56.17 and 513.85 ± 89.53 s, respectively. Vincristine polymer dissociation upon dilution, like that of

Table 3: Stopped-Flow Light Scattering with a Drug Dilution of 50to 25 μM

drug	[tubulin] μM	A1	τ (s)
vinorelbine	0.5	0.66 ± 0.10	12.77 ± 3.44
	1.0	0.99 ± 0.18	9.33 ± 1.04
	1.5	1.25 ± 0.11	7.56 ± 1.29
vinblastine	0.5	0.55 ± 0.07	34.60 ± 2.29
	1.0	0.96 ± 0.05	26.18 ± 0.33
	1.5	1.26 ± 0.10	19.97 ± 4.98

drug	[tubulin] (μM)	A1	τ_1 (s)	A2	τ_2 (s)
vincristine	0.5	1.15 ± 0.12	145.72 ± 34.54	0.86 ± 0.28	561.47 ± 56.92
	1.0	0.37 ± 0.05	51.29 ± 33.25	3.05 ± 0.17	538.73 ± 122.53
	1.5	0.51 ± 0.17	54.80 ± 18.71	2.54 ± 0.03	417.53 ± 1.20
			mean 92.76 ± 56.17		513.85 ± 89.53

Table 4: Kinetic and Drug Binding Parameters from Stopped-Flow Measurements

	k_a (M^{-1} s^{-1})	k_d (s^{-1})	K (M^{-1})	K_2 (M^{-1})[a]
vinorelbine	1.1×10^5	0.0210	5.4×10^6	1.5×10^6
vinblastine	4.2×10^5	0.0082	5.2×10^6	5.1×10^6

[a] From sedimentation velocity experiments reported here and Lobert et al. (1995).

vinblastine and vinorelbine, involves a cascade of dissociation events, albeit with exceptionally slow relaxation times. We assign τ_1 to comparable events observed with vinblastine and vinorelbine involving dissociations of heterodimers or oligomers, the increased relaxation times observed being due to the larger size distribution of vincristine-induced spirals. The second relaxation time, τ_2, suggests another event involving larger polymers or aggregates, possibly alignment of spirals or tubulin denaturation. To investigate this possibility, we carried out sedimentation velocity experiments at 4 μM tubulin, 50 μM GTP, and 50 μM vincristine (our initial conditions in the kinetic experiments were 25 °C, 10 mM Pipes, pH 6.9, 2 mM EGTA, and 1 mM $MgSO_4$). When the sample was spun at 5000 rpm, peaks were observed at 47S, 76S, 109S, and 153S, in addition to a skewed boundary near 28S. The peaks >28S represent approximately 10% of the starting material. When this sample was accelerated to 20 000 rpm, the larger material pelleted and the remaining material resolved as a single skewed boundary with a peak near 31S ($\bar{s}_{20,w}$ = 30.7S). Electron microscopy confirmed the presence of large amorphous sheets and bundles of short rods, about 100 nm in length (data not shown). This minor component of larger aggregates will dominate the observed light scattering and thus probably accounts for the second relaxation phenomenon. In sedimentation velocity experiments, these aggregates will quickly pellet and not contribute to our quantitative analysis. At 2 μM tubulin (the concentration used in the sedimentation velocity experiments; summarized in Figures 1 and 2 and Table 1), there is no evidence of significant amounts of vincristine-induced macrotubes or sheets.

DISCUSSION

Nucleotide Dependence of Vinca Alkaloid-Induced Tubulin Association. We previously demonstrated by sedimentation velocity experiments that GDP enhances vinblastine-induced tubulin self-assembly relative to GTP (Lobert et al., 1995). This enhancement is observed when we fit these data with an isodesmic ligand-mediated or ligand-mediated plus -facilitated model to obtain binding affinities. Here we report similar experiments and analysis with vinorelbine and vincristine. These new data also demonstrate a GDP enhancement for vinorelbine- and vincristine-induced tubulin assembly and strongly suggest similar behavior for all vinca alkaloid derivatives. GDP enhancement must be due to an intrinsic feature of the tubulin structure. The mean enhancement relative to GTP is 0.90 ± 0.17 kcal/mol. When 25 °C data are fit with the ligand-mediated model, the $\Delta G°$ for drug-induced tubulin association is most negative for vincristine, −17.6 and −16.9 kcal/mol in the presence of GDP and GTP, respectively, and least negative for vinorelbine, −16.5 and −15.6 kcal/mol in the presence of GDP and GTP, respectively. Our previously reported values for vinblastine fall between the values of these two drugs, −17.0 and −16.1 kcal/mol for GDP and GTP, respectively (Lobert et al., 1995). Figure 3 shows this energetic relationship graphically for all three drugs. Similar trends are found with the combined model fits at 5 and 36 °C. The difference between vincristine and vinblastine amounts to a $\Delta\Delta G°$ of 0.79 kcal/mol for data fit with the ligand-mediated model (0.64 kcal/mol for all models). The difference for the vinblastine−vinorelbine affinity amounts to a $\Delta\Delta G°$ of 0.46 kcal/mol for the ligand-mediated model (0.26 kcal/mol for all models). The binding affinity of vinorelbine, vinblastine, or vincristine for tubulin heterodimers, K_1, is identical within error for all three drugs, 1.55×10^5 (± 0.34) M^{-1} at 25 °C [Table 1 and Lobert et al. (1995)]. The major differences are in the affinity of liganded heterodimers for polymers, K_2. These results do not agree entirely with those of Prakash and Timasheff (1985), where they found a nearly 2-fold increase in K_1 for vincristine relative to that of vinblastine. Note that they also report a constrained combined fit with $K_4 = 1 \times 10^4$ M^{-1}. However, a reanalysis of the vinblastine data by Na and Timasheff (1986a) generates a K_1 value that is nearly identical to the value reported by Prakash and Timasheff (1985) for vincristine (3.8×10^4 and 3.5×10^4 M^{-1} at 0 mM Mg^{2+} for vinblastine and vincristine, respectively). Furthermore, Prakash and Timasheff (1985) found a nearly 4-fold overall enhancement, K_1K_2, induced by vincristine relative to that of vinblastine equal to a $\Delta\Delta G°$ of 0.81 kcal/mol, which also agrees quite well with our data.

We also find a 2−5-fold enhancement in K_2 for all three drugs in the presence of GDP compared to GTP. The enhancement is also found in K_3, when data are fit with the combined ligand-mediated plus -facilitated model, indicating a linkage of GDP enhancement to vinca alkaloid-induced tubulin self-association. Data collected at 5, 25, and 36 °C for vinorelbine demonstrate the same temperature depend-

ence observed with vinblastine (Lobert et al., 1995), where increasing temperature resulted in increased overall affinity, K_1K_2 (Table 1). Although vincristine sedimentation data demonstrate increasing maximum *s* values with increasing temperature (Figure 1), this temperature dependence is not reflected in K_1K_2 (Table 1). Determinations of binding affinities are dependent on the model used to fit the sedimentation data, and thus, the model chosen may result in an underestimation or an incorrect estimation of the actual binding affinities. With this in mind, we decided to investigate the mechanism of vinca alkaloid-induced tubulin self-association by stopped-flow light scattering experiments.

Mechanism of Vinca Alkaloid-Induced Tubulin Association. Stopped-flow light scattering data demonstrated that, when drug concentrations are diluted from 50 to 25 μM, vinca alkaloid-induced tubulin association occurs by a similar mechanism for all three drugs (Figure 4). Increasing tubulin concentrations resulted in decreasing relaxation times (Table 3). Thusius et al. (1975) demonstrated that, for glutamate dehydrogenase, this type of protein concentration dependence indicates self-association occurs by association of single protein subunits to the ends of polymers and by association of oligomers to form polymers, as indicated by the scheme

$$P_i + P_1 \rightleftharpoons P_{i+1}$$

$$P_i + P_j \rightleftharpoons P_k$$

We propose that, under the conditions of our experiments, oligomer association occurs when vinorelbine or vinblastine is present and most likely, it also occurs when vincristine is present, although within the error of our measurements oligomer association with vincristine remains uncertain. Vinorelbine and vinblastine data are best explained by a single relaxation phenomenon, whereas at the same tubulin concentrations, vincristine-induced tubulin association involves two or more events. The additional phenomena observed in the vincristine relaxation data could be due to tubulin denaturation. Previously, it was suggested that vincristine has a tendency to denature tubulin (Prakash & Timasheff, 1983, 1992). In order to investigate this possibility, we left tubulin samples, prepared in the presence of vincristine, on ice for 4 h before beginning our sedimentation velocity experiment at 37 °C (data not shown). We found no change in distribution of polymers or extent of association when compared to those of samples prepared and immediately centrifuged. Although samples for light scattering experiments must be degassed for 1 h prior to collecting stopped-flow data, it appears that this does not result in an appreciable amount of tubulin denaturation. Thus, it is unlikely that tubulin denaturation induced by vincristine is the cause of the additional phenomenon observed in our kinetic experiment. Note that Prakash and Timasheff (1983, 1985) worked in a Mg^{2+}-free buffer with tubulin that was isolated in the absence of reducing agents. This may partially explain their observations.

It has been suggested that paracrystal formation both *in vivo* (Fujiwara & Tilney, 1975) and *in vitro* (Na & Timasheff, 1982) in the presence of vinblastine or vincristine, as well as other antimitotic agents, is caused by the alignment of vinblastine-induced spirals. Paracrystals occur at stoichiometric drug concentrations and appear as short and rodlike structures composed of macrotubes, formed from tubulin helices packed longitudinally (Na & Timasheff, 1982; Amos et al., 1984; Nogales et al., 1995). Our relaxation kinetic experiments were carried out at initial concentrations of 50 μM drug and tubulin from 1.5 to 4 μM in the presence of 50 μM GTP. Sedimentation velocity experiments with 50 μM vincristine and 4 μM tubulin demonstrated that, although the majority of the material is in the expected skewed boundary (28S peak), larger species also occur, possibly due to the longitudinal alignment of tubulin helices. Electron microscopy revealed large sheets or bundles of polymers that could account for the second relaxation phenomenon. The large affinity of vincristine for tubulin relative to the affinity of vinblastine or vinorelbine for tubulin probably accounts for the presence of macrotubes in only the vincristine solution under our sedimentation velocity conditions. A recent study of vinblastine-induced spirals and paracrystals (Nogales et al., 1995) suggests that high Mg^{2+} concentrations diminish paracrystal formation. We found recently that high ionic strength (150 mM NaCl) completely abolishes the second slow relaxation time with vincristine (S. Lobert, C. A. Boyd, and J. J. Correia, manuscript in preparation).

Prakash and Timasheff (1983) suggested that the shape of the vincristine-induced boundary in a sedimentation velocity experiment (a single forward-skewed peak with a trailing edge) is in complete agreement with the indefinite isodesmic model as described by Holloway and Cox (1974). Note that, at low concentration ratios of drug, a bimodal pattern can be generated by a gradient of ligand caused by a depletion of drug from the meniscus (Prakash & Timasheff, 1983). This is something we never observe due to the high drug:tubulin ratios used in our work. An additional complexity that we must consider is the slow kinetics observed for all three drugs (Figure 4, Table 3). Will relaxation times of 10−90 s disturb the boundary and bias our results? Kegeles and Cann (1978) investigated the role of kinetics in a mass transport system involving ligand-mediated dimerization. They concluded that relaxation times <116 s will continue to appear in rapid equilibrium in a sedimentation velocity experiment. While this is encouraging, it is not entirely clear if this also applies to a ligand-mediated isodesmic system that is also undergoing annealing.

In order to investigate whether the kinetics of vincristine-induced tubulin association contributes to spiral polymer distributions found in sedimentation velocity experiments, we carried out sedimentation experiments in the presence of vincristine at 37 °C and varying speeds (15 000, 20 000, and 30 000 rpm) (data not shown). At lower speeds, the distributions of polymers were sharper and the peak position was shifted to slightly lower *s* values. The shapes of the sedimentation patterns appear to represent a distribution of polymers that at lower speeds have additional time to reequilibrate and show a narrower distribution. Note that vincristine at 37 °C makes the largest polymers and thus exacerbates this effect. We do not see this effect at lower temperatures or with other drugs under our experimental conditions. It is likely that the long relaxation time observed for vincristine (Figure 4) contributes to this speed-dependent effect. However, an additional factor that may contribute to the observed boundary shape in this system is heterogeneity of tubulin isotypes. Mammalian tubulin is composed of six α and seven β gene products. Porcine brain is known to be composed of four predominant β chains with associated

α-tubulin. We are currently investigating the interaction of vinca alkaloids with immunoaffinity-purified β-tubulin isotypes in sedimentation velocity experiments. We find that vincristine binds to αβ class III tubulin with lower overall affinity than to other isotypes (S. Lobert, A. Frankfurter, and J. J. Correia, manuscript in preparation), suggesting that this weaker binding may contribute to the observed centripetal tail in the vincristine sedimentation profiles. Consistent with an isodesmic mechanism, αβ class III tubulin also gives a skewed boundary shape in the presence of vincristine, suggesting that the boundary shapes observed with unfractionated PC-tubulin are a superposition of isodesmic patterns with different association constants (K_2). Note, as previously reported, we do not see the reduced binding to αβ class III with vinblastine (Lobert et al., 1995) or vinorelbine. Brain tubulin is typically 25% β class III tubulin (Banerjee et al., 1988), and thus, diminished interaction of β class III with vincristine could account for the unusual trends observed for K_1K_2 and $\Delta H°$. In general, however, the same GDP enhancement is observed with vincristine, as with vinblastine and vinorelbine, suggesting the energetics estimated by these studies are largely correct for all three drugs. Thus, we conclude that our data accurately reflect the energetics of vinca alkaloid-induced tubulin self-association, but complexities of kinetics and heterogeneity, especially for vincristine at 37 °C, do contribute to the process.

Implications for in Vivo Antitumor and Toxic Effects. The antitumor effects of vinca alkaloids occur as a result of substoichiometric drug interactions which diminish dynamic instability (Jordan & Wilson, 1990; Toso et al., 1993; Dhamodharan et al., 1995). Drug binding is thought to occur at the ends of microtubules, probably via association with the GTP cap. It has been proposed that vinca alkaloids cause spiral growth from the ends of microtubules, destabilizing lateral interactions between protofilaments (Na & Timasheff, 1982). Additionally, the GDP enhancement of tubulin association, observed first with vinblastine (Lobert et al., 1995), and now with two other vinca alkaloids, vincristine and vinorelbine, suggests that spirals may propagate into the microtubule core by a zipper-like or protofilament-peeling mechanism (Himes, 1991; Lobert et al., 1995; Dhamodharan et al., 1995). It should be noted that fluorescence quenching studies with another vinca alkaloid, vinzolidine, also showed GDP enhancement of binding affinities (Codaccioni et al., 1988), although those workers did not interpret their data in terms of an effect on self-association (Correia, 1991). These results collectively suggest that a destabilizing effect on the GDP core of microtubules is likely to be a common mechanism in vinca alkaloid chemotherapeutics. Note that our experiments are performed at 2 μM tubulin, concentrations that mimic the critical concentration for microtubule assembly *in vivo*. Thus, while it has been assumed that vinca alkaloids are interacting with microtubule ends, it is highly likely that the cellular heterodimeric tubulin pool also self-associates into spirals. Our kinetic results suggest that spirals or liganded heterodimers could associate with microtubule ends, suppressing dynamics. This possibility explains two observations made by Dhamodharan et al. (1995). First, they found that, at substoichiometric drug concentrations *in vitro* and at low drug concentrations in culture media, microtubules are observed to have relatively stable life history traces or lengths with only slow changes in length. This may correspond to a steady state version of the kinetics of polymer redistribution we observe by stopped-flow light scattering studies (Figure 4, Table 3). Gildersleeve et al. (1992) report a range of shortening rates for microtubules from 4.1 μm/min in cells to 83.6 μm/min *in vitro*, corresponding to a k_{off} of 8.4−171.5 s^{-1}. (We convert micrometers per minute by assuming 1600 subunits/μm and 13 sites of dissociation/microtubule end.) This is 10^3−10^4 faster than the k_{off} values we estimate for vinca alkaloid-induced spirals (Table 4) and consistent with the dramatic stabilizing effect vinca alkaloids have in microtubule dynamics. Second, Dhamodharan et al. (1995) observed an increase in polymer mass at low concentrations of vinblastine and ascribed it to a stabilization of microtubules during isolation. This is consistent with our kinetic data. However, it is also possible that an increase in polymer mass is partially due to addition of vinca alkaloid-induced spirals to the ends of microtubules, thus increasing the concentration of tubulin in the cytoskeletal pellet. For this mass increase to be appreciable, the affinity of vinblastine for microtubule ends must be large. If spirals grow off the ends of microtubules, then the overall affinity of vinca alkaloids for microtubule ends must correspond to the overall affinity estimated in our fits of weight average sedimentation coefficients (Table 1; Lobert et al., 1995) and corrected for cellular ionic conditions. This affinity corresponds to K_1K_2 and, although model-dependent, is much larger than previous estimates for the affinity of vinblastine for microtubule ends. Wilson et al. (1982) estimated the K_d for vinblastine binding to microtubule ends to be 2 μM by a steady state binding assay. While this is the best estimate in the literature, it probably corresponds to a K_{app} value that approximates K_1K_2. Our K_1K_2 estimates are both model- and nucleotide-dependent, but for vinblastine at 25 °C, they correspond to 0.04−0.0003 nM (Lobert et al., 1995). Taking into account that unpolymerized cellular tubulin acts as a buffer for drug binding, these estimates may be more consistent with the remarkable ability of these drugs to suppress microtubule dynamics.

In our experiments reported here, we also found that K_1, the binding of vinca alkaloids to tubulin heterodimers, is identical for vincristine, vinblastine, and vinorelbine and is not nucleotide-dependent. Additionally, we found that the overall affinities, K_1K_2, in order of magnitude are vincristine > vinblastine > vinorelbine. These results indicate that the differential effects on K_2, the affinity of liganded heterodimers for spiral polymers, and K_3, the affinity of drug for unliganded tubulin polymers, are caused by a conformational effect at a distance from the drug binding site and/or a conformational change at the drug binding site induced by tubulin self-association. How can K_1 for all three drugs be identical while K_2, manifested at some distant site, is dramatically different for the same three drugs? At first glance, this appears unusual. Certainly the allosteric effect of vinca alkaloids and GDP on spiral formation, K_2, at a distant site is understandable, as is the variation among different vinca alkaloids. One possibility to explain the constant K_1 is that other changes energetically compensate for the influence of structural changes in the drug. Thus, if modifying vinblastine to vincristine increased interactions at the binding site but also induced a conformational change unconnected to spiral formation that cost energy, then K_1 would be unperturbed. However, an alternate explanation is in the realization that an enhancement in K_2 is also manifested as an enhancement in K_3. Thus, vincristine does

in fact bind tighter than vinblastine, and vinblastine does bind tighter than vinorelbine, but only to the polymeric form. This is quite similar to the GTP enhancement of tubulin polymerization, where the difference between GTP and GDP interactions with heterodimers is minimal, but quite substantial once polymerization occurs (Correia, 1991). This interpretation is consistent with the theories of allosterism where allosteric effects are only manifested in polymeric complexes.

This is the first quantitative comparison of vincristine and vinblastine with the new antineoplastic agent vinorelbine. These data allow us to cautiously correlate the clinical doses of these agents with their overall affinity for the site of action, tubulin and microtubules. We find that the overall binding affinities, where vincristine > vinblastine > vinorelbine, correlate well with the weekly intravenous drug doses, where vincristine < vinblastine < vinorelbine (Rahmani et al., 1986). Furthermore, the absence of individual drug effects on K_1 and the observed differences in K_2 and K_3 suggest that the antitumor efficacy and drug potency are linked to tubulin self-association. This may occur because of a differential drug interaction with microtubule protofilaments or tubulin conformational differences induced by the drugs at a distance. Additional evidence for drug effects at a distance comes from studies of cross-resistance, indicating that mutations that enhance microtubule stability occur at a site different from where the antimitotics bind (Morris, 1979; Cabral et al., 1980; Keates et al., 1981). Differential effects on microtubule dynamics may correlate clinically with the amount of drug needed to suppress tumor growth. Weekly drug doses, however, are determined not only by drug potency but also by dose-limiting toxicities. Vincristine doses are limited by the drug-induced neurotoxicity, whereas vinblastine and vinorelbine doses are limited by bone marrow toxicity [reviewed in Lobert and Correia (1992)]. The longer relaxation times observed with vincristine, as well as differential binding to individual tubulin isotypes, may contribute to the neurotoxicity found clinically. To address these issues, additional information is needed comparing the affinities of vinca alkaloids for tubulin isotypes, as well as the relative amounts of tubulin isotypes in tumors and in normal tissues. These studies are currently in progress.

ACKNOWLEDGMENT

We thank Alex Slawson, Sandor Varadi, and Coleman Boyd for technical assistance with these experiments. We are grateful to Pelahatchie Country Meat Packers for providing pig heads for tubulin purification.

REFERENCES

Amos, L. A., Jubb, J. S., Henderson, R., & Vigers, G. (1984) *J. Mol. Biol. 178*, 711−729.

Banerjee, A., Roach, M. C., Wall, K. A., Lopata, M. A., Cleveland, D. W., & Luduena, R. F. (1988) *J. Biol. Chem. 263*, 3029−3034.

Bernasconi, C. F. (1976) *Relaxation Kinetics*, Academic Press, New York.

Binet, S., Chaineau, E., Fellous, A., Lataste, H., Krikorian, A., Couzinier, J. P., & Meininger, V. (1990) *Int. J. Cancer 46*, 262−266.

Cabral, F., Sobel, M. E., & Gottesman, M. M. (1980) *Cell 20*, 29−36.

Codaccioni, F., Dell'Amico, M., Bourdeaux, M., Briand, C., & Lux, B. (1988) *Arch. Biochem. Biophys. 267*, 236−244.

Correia, J. J. (1991) *Pharmacol. Ther. 52*, 127−147.

Correia, J. J., Baty, L. T., & Williams, R. C., Jr. (1987) *J. Biol. Chem. 262*, 17278−17284.

Detrich, H. W., & Williams, R. C., Jr. (1978) *Biochemistry 17*, 3900−3907.

Dhamodharan, R., Jordan, M. A., Thrower, D., Wilson, L., & Wadsworth, P. (1995) *Mol. Biol. Cell 6*, 1215−1229.

Fellous, A., Chayon, R., Vacassin, T., Binet, S., Lataste, H., Krikorian, A., Couxinier, J. P., & Meininger, V. (1989) *Semin. Oncol. 16*, 9−14.

Fujiwara, K., & Tilney, L. G. (1975) *Ann. N. Y. Acad. Sci. 253*, 27−50.

Gildersleeve, R. F., Cross, A. R., Cullen, K. E., Fagen, A. P., & Williams, R. C., Jr. (1992) *J. Biol. Chem. 267*, 7995−8006.

Himes, R. H. (1991) *Pharmacol. Ther. 51*, 257−267.

Holloway, R. R., & Cox, D. J. (1974) *Arch. Biochem. Biophys. 160*, 595−602.

Jordan, M. A., & Wilson, L. (1990) *Biochemistry 29*, 2730−2739.

Jordan, M. A., Thrower, D., & Wilson, L. (1991) *Cancer Res. 51*, 2212−2222.

Keates, R. A. B., Sarangi, F., & Ling, V. (1982) *Proc. Natl. Acad. Sci. U.S.A. 78*, 5638−5642.

Kegeles, G., & Caan, J. R. (1978) *Methods Enzymol. 48*, 248−270.

Liu, S., & Stafford, W. F., III (1995) *Anal. Biochem. 224*, 199−202.

Lobert, S., & Correia, J. J. (1992) *Cancer Nurs. 15*, 22−33.

Lobert, S., Frankfurter, A., & Correia, J. J. (1995) *Biochemistry 34*, 8050−8060.

Morris, N. R., Lai, M. H., & Oakley, C. E. (1979) *Cell 16*, 437−442.

Na, G. C., & Timasheff, S. N. (1982) *J. Biol. Chem. 257*, 10387−10391.

Na, G. C., & Timasheff, S. N. (1986a) *Biochemistry 25*, 6214−6222.

Na, G. C., & Timasheff, S. N. (1986b) *Biochemistry 25*, 6222−6228.

Nogales, E., Medrano, F. J., Diakun, G. P., Mant, G. R., Towns-Andrews, E., & Bordas, J. (1995) *J. Mol. Biol. 254*, 416−430.

Owellen, R. J., Owens, A. H., Jr., & Donigan, D. W. (1972) *Biochem. Biophys. Res. Commun. 47*, 685−691.

Prakash, V., & Timasheff, S. N. (1983) *J. Biol. Chem. 258*, 1689−1697.

Prakash, V., & Timasheff, S. N. (1985) *Biochemistry 24*, 5004−5010.

Prakash, V., & Timasheff, S. N. (1992) *Arch. Biochem. Biophys. 295*, 137−145.

Rahmani, R., Gueritte, F., Martin, M., Just, S., Cano, J. P., & Barbet, J. (1986) *Cancer Chemother. Pharmacol. 16*, 223−228.

Stafford, W. F., III (1992a) *Anal. Biochem. 203*, 295−301.

Stafford, W. F., III (1992b) in *Analytical Ultracentrifugation in Biochemistry and Polymer Science* (Harding, S. E., Rowe, A. J., & Horton, J. C., Eds.) pp 359−393, Royal Society of Chemistry, Cambridge.

Stafford, W. F., III (1994) in *Methods in Enzymology. Numerical Computer Methods, Part B.* (Johnson, M. L., & Brand, L., Eds.) pp 478−501, Academic Press, New York.

Thusius, D., Dessen, P., & Jallon, J. M. (1975) *J. Mol. Biol. 92*, 413−432.

Toso, R. J., Jordan, M. A., Farrell, K. W., Matsumoto, B., & Wilson, L. (1993) *Biochemistry 32*, 1285−1293.

Williams, R. C., Jr., & Lee, J. C. (1982) *Methods Enzymol. 85*, 376−408.

Wilson, L., Jordan, M. A., Morse, A., & Margolis, R. L. (1982) *J. Mol. Biol. 159*, 125−149.

BI953037I